

ACCEPTED MANUSCRIPT

Infrared Nano-Imaging of Electronic Phase across the Metal-Insulator Transition of NdNiO₃ Films

To cite this article before publication: Fanwei Liu *et al* 2022 *Chinese Phys. Lett.* in press <https://doi.org/10.1088/0256-307X/39/7/076801>

Manuscript version: Accepted Manuscript

Accepted Manuscript is “the version of the article accepted for publication including all changes made as a result of the peer review process, and which may also include the addition to the article by IOP Publishing of a header, an article ID, a cover sheet and/or an ‘Accepted Manuscript’ watermark, but excluding any other editing, typesetting or other changes made by IOP Publishing and/or its licensors”

This Accepted Manuscript is © 2022 Chinese Physical Society and IOP Publishing Ltd.

During the embargo period (the 12 month period from the publication of the Version of Record of this article), the Accepted Manuscript is fully protected by copyright and cannot be reused or reposted elsewhere.

As the Version of Record of this article is going to be / has been published on a subscription basis, this Accepted Manuscript is available for reuse under a CC BY-NC-ND 3.0 licence after the 12 month embargo period.

After the embargo period, everyone is permitted to use copy and redistribute this article for non-commercial purposes only, provided that they adhere to all the terms of the licence <https://creativecommons.org/licenses/by-nc-nd/3.0>

Although reasonable endeavours have been taken to obtain all necessary permissions from third parties to include their copyrighted content within this article, their full citation and copyright line may not be present in this Accepted Manuscript version. Before using any content from this article, please refer to the Version of Record on IOPscience once published for full citation and copyright details, as permissions will likely be required. All third party content is fully copyright protected, unless specifically stated otherwise in the figure caption in the Version of Record.

View the [article online](#) for updates and enhancements.

Infrared Nano-Imaging of Electronic Phase across the Metal-Insulator Transition of NdNiO₃ Films

Fanwei Liu()^{1†}, Sisi Huang()^{2†}, Sidan Chen()¹, Xinzhong Chen()³,
Mengkun Liu()³, Kuijuan Jin()^{2*} and Xi Chen()^{1*}

¹State Key Laboratory of Low Dimensional Quantum Physics and Department of Physics,
Tsinghua University, Beijing 100084, China

²Institute of Physics, Chinese Academy of Sciences, Beijing 100190, China

³Department of Physics and Astronomy, Stony Brook University, Stony Brook, NY 11794, USA

NdNiO₃ is a typical correlated material with temperature-driven metal-insulator transition. Resolving the local electronic phase is crucial in understanding the driving mechanism behind the phase transition. Here we present a nano-infrared study of the metal-insulator transition in NdNiO₃ films by a cryogenic scanning near-field optical microscope. The NdNiO₃ films undergo a continuous transition without phase coexistence. The nano-infrared signal shows significant temperature dependence and a hysteresis loop. Stripe-like modulation of the optical conductivity is formed in the films and can be attributed to the epitaxial strain. These results provide valuable evidence to understand the coupled electronic and structural transformations in NdNiO₃ films at the nano-scale.

PACS: 68.37.Uv, 71.30.+h, 78.20.-e

DOI:

Perovskite rare-earth nickelates (RNiO₃) are correlated electron systems with charge-transfer type metal-insulator transition (MIT) driven by temperature^[1–3]. The mechanism of MIT in RNiO₃ involves electronic, magnetic and lattice degrees of freedom^[4–6] and is still under debate. The detailed behavior depends on the species of the rare-earth R ion. With decreasing temperature, the transition from a paramagnetic metal to an insulator occurs at T_{MIT} ^[7–10]. A charge order also appears in the insulating phase. At the Neel temperature $T_N \leq T_{MIT}$, the spin structure becomes antiferromagnetic.

As a well-studied member of the RNiO₃ family, NdNiO₃ (Fig.1(a)) undergoes the metal-to-insulator and paramagnetic-to-antiferromagnetic transitions simultaneously^[11–12], i.e., $T_N = T_{MIT}$. The metal-insulator transition is also accompanied by a structural change from orthorhombic ($Pbnm$) to monoclinic ($P2_1/n$) symmetry^[12–13]. During the structure transition, the NiO₆ octahedra distorts and rotates. Compared with bulk NdNiO₃, epitaxial strain and finite film thickness result in more complications during phase transition in films^[14–16]. So far, most data about NdNiO₃ films was acquired by macroscopic measurements. Nevertheless more and more evidence indicates that the material exhibits strong spatial inhomogeneity at the nano-scale and microscopy is essential to elucidate the MIT mechanism. For example, recent works^[17–19] demonstrate the nano-scale phase coexistence when the NdNiO₃ films go through the first-order metal-insulator phase transitions. The phase transition is broadened by disorder such as strain field and therefore occurs over a finite range of temperatures where the fraction of low-temperature phase grows from zero to one as the temperature is lowered. Here we report another scenario that features a continuous transition without phase coexistence when NdNiO₃ films go through the metal-insulator transition. The nano-infrared (nano-IR) study is performed on a scattering-type scanning near-field microscope (s-SNOM). Such infrared near-field microscopy probes local optical conductivity with nanometer resolution^[20–21] and has been successfully applied to the investigation of correlated oxides^[22–24].

The NdNiO₃ films were deposited on the (100)-oriented cubic (LaAlO₃)_{0.3}(Sr₂AlTaO₆)_{0.7} (LSAT, $a = 0.3868$ nm) substrates by pulsed laser deposition (PLD). The pseudo-cubic perovskite lattice parameter of bulk NdNiO₃ is estimated to be 0.3807 nm^[2]. The in-plane lattice mismatch is $+1.6\%$. Compared with NdNiO₃ films grown on (110)-oriented NdGaO₃ substrates, the NdNiO₃ films on the LSAT substrates are under a larger tensile strain^[16]. During the film deposition, the LSAT substrate was kept at 650 °C under an oxygen atmosphere of 20 Pa. Then the sample was annealed at room temperature under an

[†]These authors contributed equally to this work.

*Corresponding author. Email: kjjin@iphy.ac.cn; xc@mail.tsinghua.edu.cn

© 2022 Chinese Physical Society and IOP Publishing Ltd

oxygen pressure of ~ 0.01 Pa. The film surface is reasonably flat (see the topography image in Fig. 1(b)) and the RMS roughness is less than 0.5 nm. Fig. 1(c) shows the resistance versus temperature ($R - T$) curve of the 15 nm thick NdNiO₃ film measured by the conventional four-probe method. The first-order transition between orthorhombic and monoclinic symmetry is smeared likely because of the strain field from the substrate. The warming and cooling cycles form a hysteresis loop. The transition occurs over a finite range of temperature from 130 K to 200 K. The resistance at low temperature exponentially depends on temperature, indicating that the film is in the insulating phase. The $R - T$ curve suggests that the first-order metal-insulator transition has been broadened by disorder^[25] and the thermal cycles should undergo various meta-stable states along the hysteresis loop. However, the transport measurement does not cover the issue of phase coexistence during the transition, which will be addressed by s-SNOM in this letter.

We employ a cryogenic s-SNOM to investigate the evolution of local electronic properties of NdNiO₃ films with temperature. The s-SNOM simultaneously maps the surface morphology and local optical response at the 20 nm scale. The CO₂ laser (p-polarized, $\lambda = 10.26 \mu\text{m}$) is focused on the atomic force microscope (AFM) tip. The mid-IR excitation at 10.26 μm probes dominantly the free-carrier Drude response of NdNiO₃ in accordance with far-field spectroscopy^[26–27]. The AFM tip is tapping at frequency Ω with an amplitude of ~ 50 nm. The local optical response is contained in the scattered signal. The higher harmonics of Ω in the signal, i.e., S_n ($n = 2, 3, \dots$), are demodulated by a lock-in amplifier (Zurich Instruments, HF2LI) to suppress the far-field background. The self-homodyne detection is used in the nano-IR imaging. Considering its nearly perfect reflectivity in the infrared frequencies^[28], 100 nm gold film is deposited at the sample edge as the reference material to quantify the local optical response.

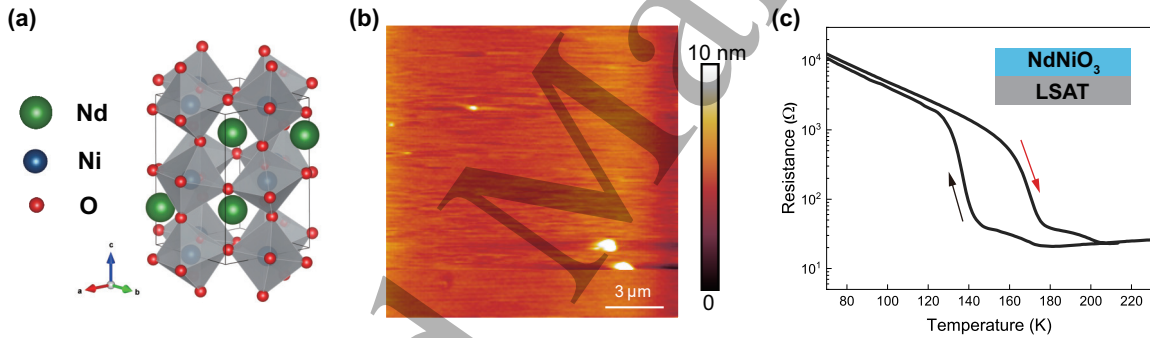


Fig. 1. (a) Crystal structure of bulk NdNiO₃. (b) AFM topography^[29] of NdNiO₃ film with 15 nm thickness at 85 K. (c) Resistance versus temperature from the transport measurement in 15 nm NdNiO₃ film. Arrows indicate the direction of transitions on warming (red) and cooling (black).

Fig. 2(a) presents the thermal cycle of the infrared nano-imaging for the same region. The spatial average \bar{S} of the near-field signal normalized by gold ($S = S_2(\text{NdNiO}_3)/S_2(\text{Au})$) shows significant temperature dependence and a hysteresis loop (Fig. 2(b)). At the ends of the loop, $\bar{S} = 0.15$ and 0.34, respectively, corresponding to the insulating and conducting phases. The near-field signal is almost homogeneous when the phase transition is completed. During the transition, the inhomogeneity of S is illustrated by the histogram in Fig. 2(c). For each temperature, the counts of pixel as a function of S shows a single peak centered at \bar{S} . The peak width is maximized at 150 K and approaches to zero at the end points of the hysteresis in Fig. 1(c). No double-peak structure signifying phase coexistence is observed in the histogram. The inhomogeneity in nano-IR signal distribution only manifests the local fluctuation of conductivity.

The local conductivity fluctuation is more pronounced in the relative nano-IR signal derived from Fig. 2(a). For each temperature of the warming cycle, the image of ΔS ($\Delta S = S - \bar{S}$) is shown in Fig. 3(a) (more data in Fig. S1 and S2). The full range of the color scale is set to $\pm 15\%$ of \bar{S} . The images of S_3 are also shown in Fig. S3 in the supplementary information. S_2 is similar to S_3 in the relative signal but with larger absolute magnitude. The stripe-like inhomogeneity along the (011) direction begins to emerge at the onset of phase transition on the $R - T$ curve and eventually disappears at the other end point of the hysteresis. The characteristic width of the stripes is about 2 μm . We propose that the stripe-like

modulation is most likely given rise by the balance between the strain energy due to inhomogeneity in the structure during the process of phase transition and that exerted by the substrate. The substrate tends to hinder the phase transition. The competition favors a less uniform distribution of structural transition and slows down the distortion and rotation of octahedra. The frustrated structural change gradually opens or closes the energy gap in the electronic band, leading to a second-order-like metal-insulator phase transition. During the thermal cycle, the stripe-like modulation remains the same but the intensity evolves with temperature (see Fig. 3(b)). We suggest that the evolution of intensity experiences various meta-stable states pinned by disorder in the process of structural transition, which is responsible for the hysteresis. More theoretical investigation is needed to confirm the above model.

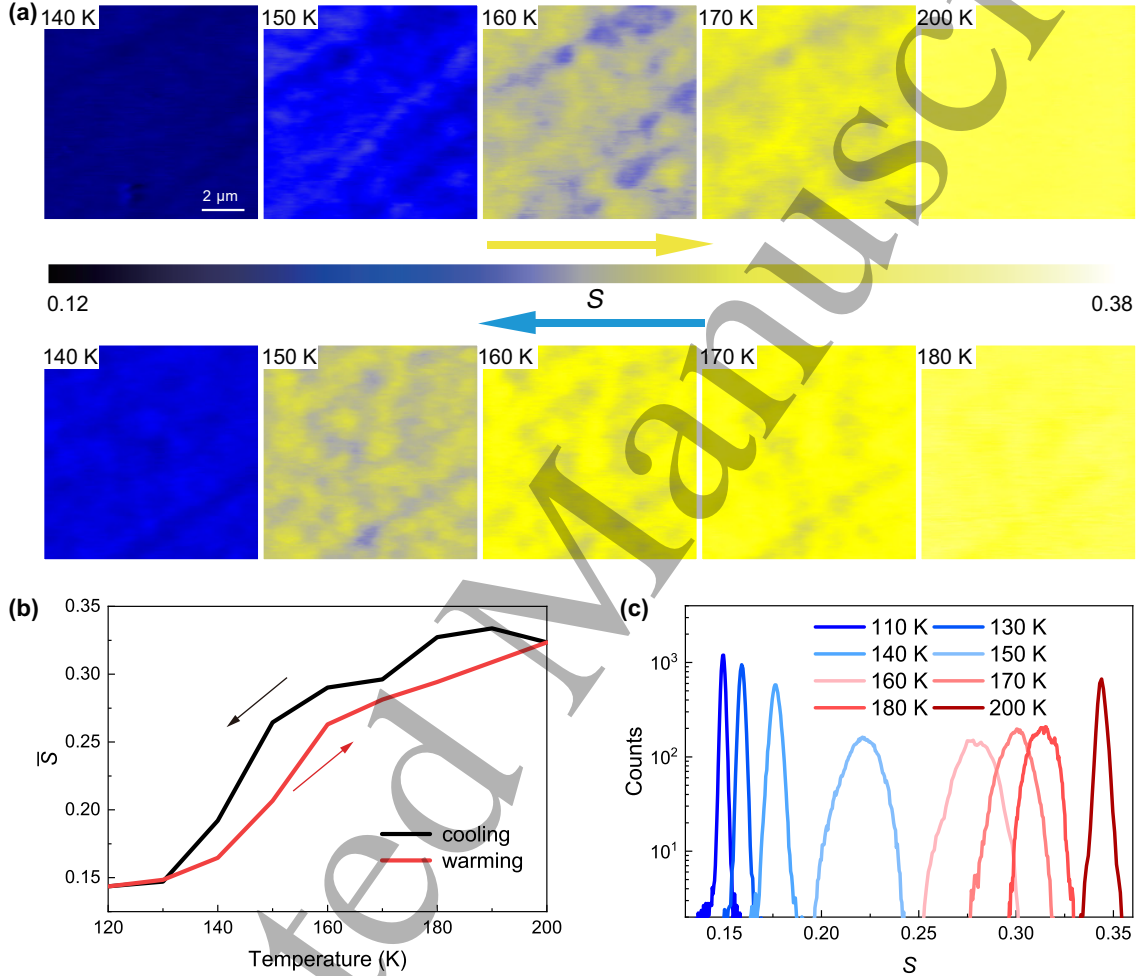


Fig. 2. (a) Images of the normalized nano-IR signal (S) acquired from NdNiO₃ film with 15 nm thickness during the warming (top) and cooling (bottom) transition. (b) The spatial average \bar{S} of nano-IR signal through the MIT. Arrows indicate the warming (red) and cooling (black) transition. (c) Histogram representation of the normalized nano-IR signal (S) on warming from 110 K to 200 K.

To demonstrate that the above observation generally presents in the NdNiO₃ thin films, we perform the experiments with different film thicknesses. Fig. 4(a) shows the $R - T$ curve for a 7 nm NdNiO₃ film on LSAT prepared under the same growth condition as that of the 15 nm film. The two kinks around 160 K on the $R - T$ curve may be related to an additional phase transition and are still not well-understood. The infrared nano-imaging (Fig. 4(b)) and the relative intensity map (Fig. 4(c) and Fig. S4) of the 7 nm film show similar modulation as those of the 15 nm film. The spatial average \bar{S} of the near-field signal normalized by gold ($S = S_2(\text{NdNiO}_3)/S_2(\text{Au})$) exhibits a hysteresis loop (Fig. 4(d)). The temperatures for the end points of the near-field signal loop are close to those of the $R - T$ loop. The loop from 155 K to 190 K is wider than that from 130 K to 155 K possibly as a result of the kinks at 160 K. Once again no indication of phase coexistence is revealed in the histogram for various temperatures (Fig. 4(e)).

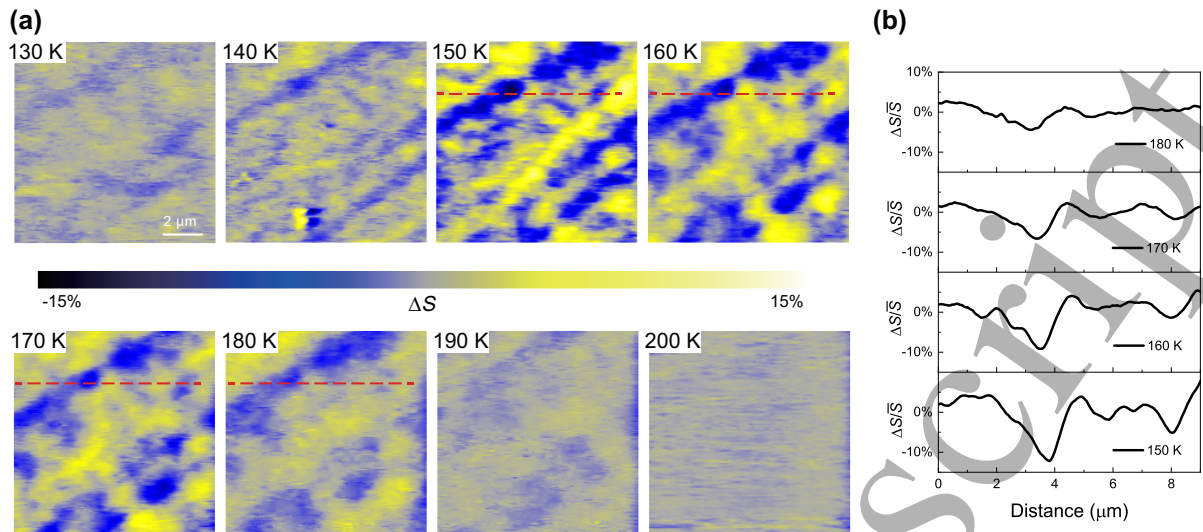


Fig. 3. (a) Images of relative nano-IR signal ($\Delta S = S - \bar{S}$) during the warming transition from NdNiO₃ film with 15 nm thickness. All images were acquired in the same field of view. (b) Line profiles (red dashed lines in (a) from 150 K to 180 K) showing the intensity of relative nano-IR signal (ΔS is normalized by \bar{S}).

Accepted Manuscript

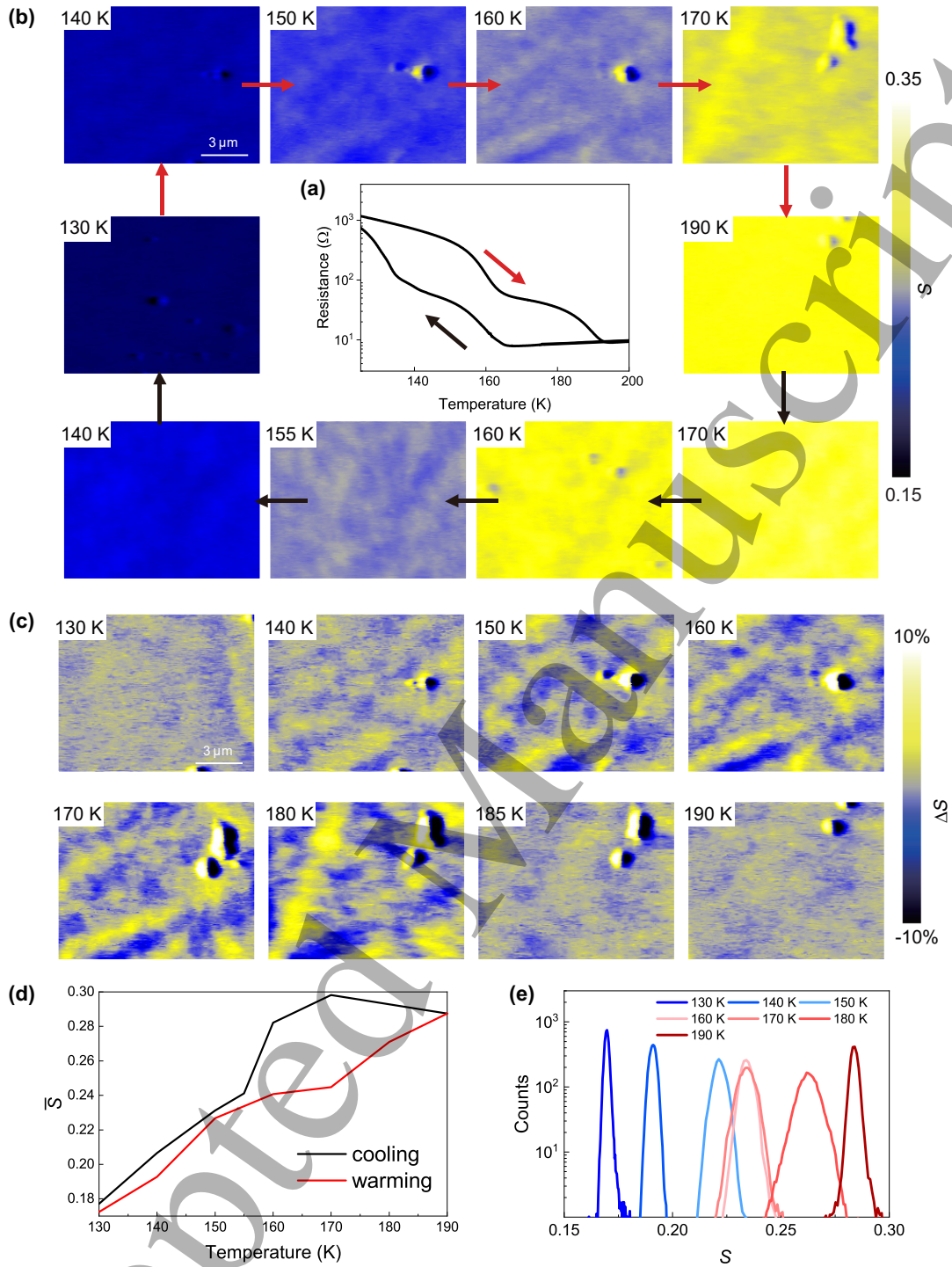


Fig. 4. (a) Temperature dependence of resistance acquired from NdNiO₃ films with 7 nm thickness. Arrows indicate the warming (red) and cooling (black) transition. (b) Images of normalized nano-IR signal (S) on warming (red arrows) and cooling (black arrows). (c) Images of relative nano-IR signal (ΔS) on warming. (d) The spatial average \bar{S} of nano-IR signal through the MIT. Inset: A zoomed-in image shows the hysteresis feature below 155 K. (e) Histogram representation of the normalized nano-IR signal (S) during the warming transition.

In summary, we demonstrate the phase transition in the correlated material NdNiO₃ at cryogenic temperature by s-SNOM. The NdNiO₃ films on the LSAT substrate undergo a continuous transition without phase coexistence across the MIT. Such observation is different from the previous studies and could be due to the different substrates. The emerging stripe-like modulation of optical conductivity during the phase transition is attributed to the hindered structural change. Our study provides new insights into the interplay between electronic and structural degrees of freedom in NdNiO₃ films.

References

- [1] Torrance J B, Lacorre P, Nazzal A I, Ansaldo E J and Niedermayer C 1992 *Physical Review B* **45** 8209
- [2] Medarde M L 1997 *Journal of Physics: Condensed Matter* **9** 1679
- [3] Catalan G 2008 *Phase Transitions* **81** 729
- [4] Alonso J A, García-Muñoz J L, Fernández-Díaz M T, Aranda M A G, Martínez-Lope M J and Casais M T 1999 *Physical Review Letters* **82** 3871
- [5] Johnston S, Mukherjee A, Elfimov I, Berciu M and Sawatzky G A 2014 *Physical Review Letters* **112** 106404
- [6] Bisogni V, Catalano S, Green R J, Gibert M, Scherwitzl R, Huang Y, Strocov V N, Zubko P, Balandeh S, Triscone J-M, Sawatzky G and Schmitt T 2016 *Nature Communications* **7** 1
- [7] Lee S, Chen R and Balents L 2011 *Physical Review Letters* **106** 016405
- [8] Middey S, Chakhalian J, Mahadevan P, Freeland J W, Millis A J and Sarma D D 2016 *Annual Review of Materials Research* **46** 305
- [9] Ruppen J, Teyssier J, Ardizzone I, Peil O E, Catalano S, Gibert M, Triscone J-M, Georges A and Van Der Marel D 2017 *Physical Review B* **96** 045120
- [10] Mercy A, Bieder J, Íñiguez J and Ghosez P 2017 *Nature Communications* **8** 1
- [11] Caviglia A D, Först M, Scherwitzl R, Khanna V, Bromberger H, Mankowsky R, Singla R, Chuang Y-D, Lee W S, Krupin O, Schlotter W F, Turner J J, Dakovski G L, Minitti M P, Robinson J, Scagnoli V, Wilkins S B, Cavill S A, Gibert M, Gariglio S, Zubko P, Triscone J-M, Hill J P, Dhessi S S and Cavalleri A 2013 *Physical Review B* **88** 220401
- [12] Gawryluk D J, Klein Y M, Shang T, Sheptyakov D, Keller L, Casati N, Lacorre Ph, Fernández-Díaz M T, Rodríguez-Carvajal J and Medarde M 2019 *Physical Review B* **100** 205137
- [13] Zhang J Y, Kim H, Mikheev E, Hauser A J and Stemmer S 2016 *Scientific Reports* **6** 1
- [14] Catalan G, Bowman R M and Gregg J M 2000 *Physical Review B* **62** 7892
- [15] Xiang P H, Zhong N, Duan C G, Tang X D, Hu Z G, Yang P X, Zhu Z Q and Chu J H 2013 *Journal of Applied Physics* **114** 243713
- [16] Liu J, Kargarian M, Kareev M, Gray B, Ryan P J, Cruz A, Tahir Nadeem, Chuang Y D, Guo J H, Rondinelli J M, Freeland J W, Fiete G A and Chakhalian J 2013 *Nature Communications* **4** 1
- [17] Mattoni G, Zubko P, Maccherozzi F, van der Torren A J, Boltje D B, Hadjimichael M, Manca N, Catalano S, Gibert M, Liu Y, Aarts J, Triscone J-M, Dhessi S S and Caviglia A D 2016 *Nature Communications* **7** 1
- [18] Preziosi D, Lopez-Mir L, Li X, Cornelissen T, Lee J H, Trier F, Bouzehouane K, Valencia S, Gloter A, Barthélémy A and Bibes M 2018 *Nano Letters* **18** 2226
- [19] Post K W, McLeod A S, Hepting M, Bluschke M, Wang Y, Cristiani G, Logvenov G, Charnukha A, Ni G X, Radhakrishnan Padma, Minola M, Pasupathy A, Boris A V, Benckiser E, Dahmen K A, Carlson E W, Keimer B and Basov D N 2018 *Nature Physics* **14** 1056
- [20] Qazilbash M M, Brehm M, Chae B G, Ho P C, Andreev G O, Kim B J, Yun S J, Balatsky A V, Maple M B, Keilmann F, Kim Hyun-Tak and Basov D N 2007 *Science* **318** 1750
- [21] Atkin J M, Berweger S, Jones A C and Raschke M B 2012 *Advances in Physics* **61** 745
- [22] Liu M K, Wagner M, Abreu E, Kittiwatanakul S, McLeod A, Fei Z, Goldflam M, Dai S, Fogler M M, Lu J, Wolf S A, Averitt R D and Basov D N 2013 *Physical Review Letters* **111** 096602
- [23] McLeod A S, Van Heumen E, Ramirez J G, Wang S, Saerbeck T, Guenon S, Goldflam M, Anderegg L, Kelly P, Mueller A, Liu M K, Schuller Ivan K and Basov D N 2017 *Nature Physics* **13** 80.
- [24] McLeod A S, Zhang J, Gu M Q, Jin F, Zhang G, Post K W, Zhao X G, Millis A J, Wu W B, Rondinelli J M, Averitt R D and Basov D N 2020 *Nature Materials* **19** 397
- [25] Kumar D, Rajeev K P, Kushwaha A K and Budhani R C 2010 *Journal of Applied Physics* **108** 063503
- [26] Katsufuji T, Okimoto Y, Arima T, Tokura Y and Torrance J B 1995 *Physical Review B* **51** 4830
- [27] Stewart M K, Liu J, Kareev M, Chakhalian J and Basov D N 2011 *Physical Review Letters* **107** 176401
- [28] McLeod A S, Kelly P, Goldflam M D, Gainsforth Z, Westphal A J, Dominguez G, Thiemens M H, Fogler M M and Basov D N 2014 *Physical Review B* **90** 085136
- [29] Nečas D, Klapetek P 2012 *Central European Journal of Physics* **10** 181

Supplementary Information for “Infrared Nano-Imaging of Electronic Phase across the Metal-Insulator Transition of NdNiO₃ Films”

Fanwei Liu()^{1†}, Sisi Huang()^{2†}, Sidan Chen()¹, Xinzhong Chen()³,
Mengkun Liu()³, Kuijuan Jin()^{2*} and Xi Chen()^{1*}

¹State Key Laboratory of Low Dimensional Quantum Physics and Department of Physics,
Tsinghua University, Beijing 100084, China

²Institute of Physics, Chinese Academy of Sciences, Beijing 100190, China

³Department of Physics and Astronomy, Stony Brook University, Stony Brook, NY 11794, USA

Cryogenic near-field optical microscope The homemade AFM assembly (including the parabolic mirror focusing the incident laser light) is mounted on the cooling stage of cryostat (Cryovac). The base temperature of the AFM assembly is 85 K with a liquid nitrogen bath. All measurements were conducted in an ultra-high vacuum ($< 10^{-9}$ mbar) environment to prevent the surface contamination (such as accumulation of dirt and impurity).

Drift control We use a fiber-coupled interferometer (attocube, LDM1300) to monitor the oscillation of tip. The probes we use are commercially available from Nanoworld (ArrowTM NCPt). The drift of tip oscillation amplitude is about 5% in an hour at 85 K. A DC bias could be applied on the Z-axis piezo-stacks of the tip step motor to continuously adjust the tip position in the range of 100 nm. When the tip position is out of the adjustment range of the DC bias, the step motors are used to recover the amplitude.

The challenges for imaging include changes in piezoelectric response of the sample scanner and thermal drift of the sample stage relative to the tip at variable temperatures. We use the standard testing sample TGQ1 (NT-MDT) for the calibration of the imaging distortion at variable temperatures. The position of the sample can be manually adjusted at different temperature. A raw scanning range is often larger than the area of the subsequent statistical measure. By tracking the pixels of the impurities, we can tailor and correct the raw images to acquire signal from the same area at different temperatures.

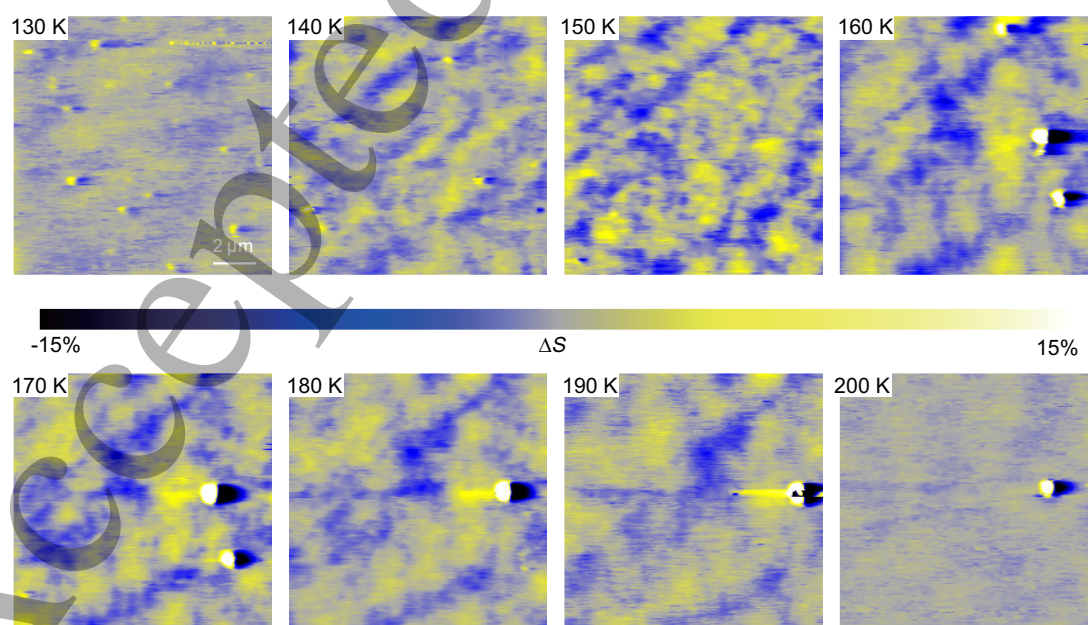


Fig. S1. More images of relative nano-IR signal (ΔS) on warming of NdNiO₃ films with 15 nm thickness.

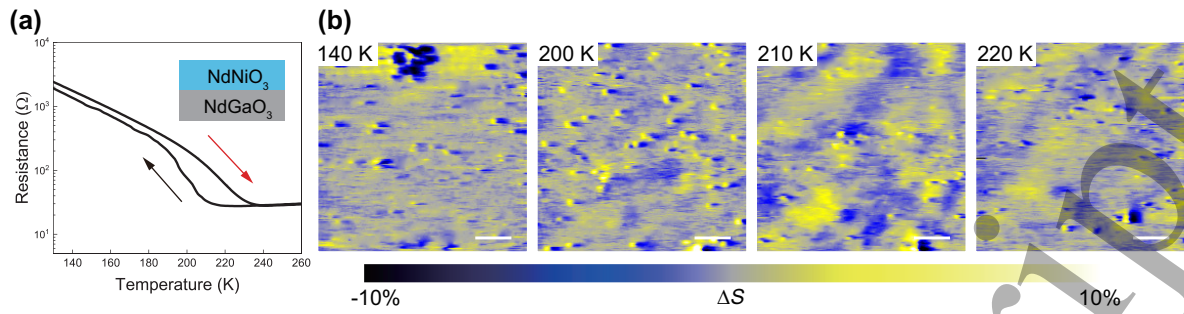


Fig. S2. NdNiO₃ films with 15 nm thickness on (100)-oriented NdGaO₃ substrate. The in-plane lattice mismatch is +1.8%. (a) Resistance versus temperature from the transport measurement. Arrows indicate the direction of transitions on warming (red) and cooling (black). (b) Images of relative nano-IR signal (ΔS) on warming in the NdNiO₃ films with 15 nm thickness. The stripe-like modulation is formed during the phase transition near 210 K.

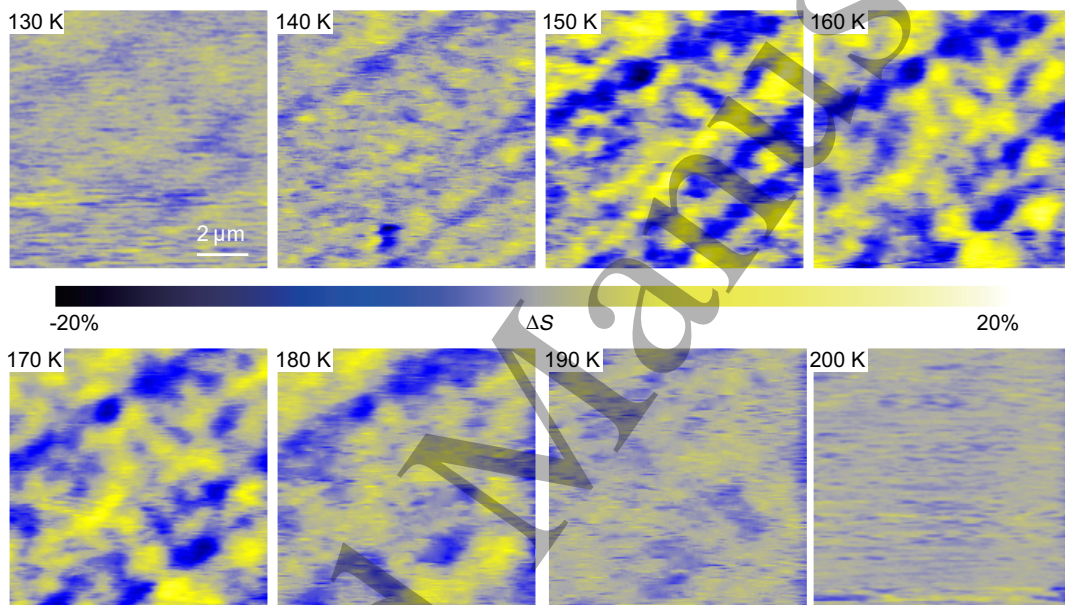


Fig. S3. Images of relative third harmonic nano-IR signal during the warming transition in NdNiO₃ films with 15 nm thickness. As a comparison with relative second harmonic nano-IR signal in the same field of view shown in Fig. 3(a).

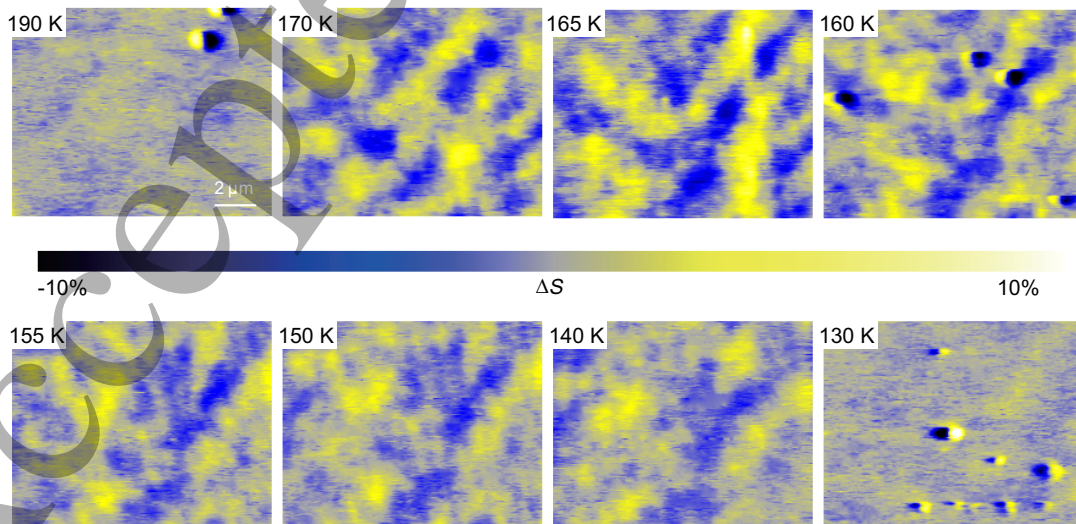


Fig. S4. Images of relative nano-IR signal (ΔS) on cooling in NdNiO₃ films with 7 nm thickness.